

## Combining 3D run-length encoding coding and searching techniques for medical image compression

Arif Sameh Arif<sup>1</sup>, Muntaha Abood Jassim<sup>2</sup>

<sup>1</sup>Department of Computer Systems Techniques, Institute of Administration Al Russaffa, Middle Technical University, Baghdad, Iraq

<sup>2</sup>Department of Basic Science, College of Density, Al Mustansiriya University, Baghdad, Iraq

### Article Info

#### Article history:

Received Apr 25, 2021

Revised Nov 11, 2021

Accepted Nov 30, 2021

#### Keywords:

3D RLE coding

Medical image compression

RLE coding

### ABSTRACT

The field of image compression became a mandatory tool to face the increasing and advancing production of medical images, besides the inevitable need for smaller size of medical images in telemedicine systems. In spite of its simplicity, run-length encoding (RLE) technique is a considerably effective and practical tool in the field of lossless image compression. Such that, it is widely recommended for 2D space that utilizes common searching techniques like linear and zigzag. This paper adopts a new algorithm taking advantage of the potential simplicity of the run-length algorithm to contribute a volumetric RLE approach for binary medical data in the 3D form. The proposed volumetric-RLE (VRLE) algorithm differs from the 2D RLE approach utilizing correlations of intra-slice only, which is used for compressing binary medical data utilizing voxel-correlations of inter-slice. Furthermore, several forms of scanning are used to extending proposed technique like Hilbert and Perimeter, which determines the best possible procedure of scanning suitable for data morphology considering the segmented organ. This work employs proposed algorithm on four image datasets to get as sufficient as possible evaluation. Experimental results and benchmarking illustrate that the performance of the proposed technique surpasses other state-of-the-art techniques with 1:30 enhancement on average.

This is an open access article under the [CC BY-SA](https://creativecommons.org/licenses/by-sa/4.0/) license.



### Corresponding Author:

Arif Sameh Arif

Department of Computer Systems Techniques, Institute of Administration Al Russaffa, Middle Technical University

Baghdad, Iraq

Email: arifsameh@ieee.org, Dr.ArifSameh2016@mtu.edu.iq

## 1. INTRODUCTION

Emerging techniques and devices used in medical image production provides increasing types of such images, which leads to higher dimension, resolution and bit depth. In other words, they produce bigger sizes of stored or transmitted image over telemedicine applications. There are different modalities of medical imaging such as thermography, positron emission tomography (PET), computed tomography (CT) and magnetic resonance imaging (MRI) that have the ability of generating (3D) images in high resolution. As example, due to high image size of color images [1], 3D CT scanner produces volumetric images that consume huge size reaching dozens of gigabytes sometimes. Such huge amounts of data need extra abilities of processing, storage and transmission over telemedicine and different centers of health care, which still considered as a challenging task despite of modern systems of communication and increasing storage abilities. As a result, image compression techniques are needed to be applied on such medical data for efficient size-reduction.



Image compression is generally divided into two types, lossy and lossless compression techniques. While lossless image compression techniques allow reconstructing compressed data perfectly, i. e. exactly as they were before compression, reconstructed images from lossy compression techniques with some degradation or lost details. This is acceptable in wide area of application but not in medical image compression, whereas they may lead to unreal diagnosis or catastrophic effects sometimes [2]. Accordingly, lossy compression methods attracted less preference in medical application of data compression regardless higher compression ratios they achieve.

Over recent years, lossless compression techniques attracted increasing attention for image compression in medical approaches [2], [3], where it was handled in several studies [3], [4]. Regarding state-of-the-art in the field of lossless compression, published algorithms provided considerable results for the compression of binary and gray-scaled images [5], [6]. Their techniques proposed different algorithms to enhance the yielded compression performance. The standard joint photographic experts group (JPEG) designed for lossy compression, and the joint photographic experts group-lossless standard (JPEG-LS) proposed for lossless compression utilized correlations between intra-slice only. So that, they obtained the redundancy of inter-pixels while using Golomb codes for data segmentation and run length encoding (RLE) to encode the data [4]. Other general standards are currently used in medical applications for binary image compression such as context adaptive lossless image compression (CALIC), octree [7], [8] and joint bilevel image experts group (JBIG) standard [9]. The standard RLE algorithm is widely employed for effective compression in modern systems due to its combination between simplicity and efficiency in symbol mapping [9]–[12].

In another study for telemetry data [13], the authors utilized the oversampling with RLE algorithm for higher efficiency in compression performance. Galloway [14] depended on RLE algorithm to attain higher compression ratio for the structure of homogeneously spread data such as in binary and grey-scale images, which contain wide areas of uniform texture. The RLE is exploited in JPEG-LS using suitable procedure of context classification to code constant image regions [15]. In the same context, RLE is jointly optimized using an iterative algorithm, which leads to better compression performance using JPEG [16]. Liaghati and Pan [17] reported the considerable performance of RLE that yield notable influence in the general performance of the compression comparing with JBIG2 and arithmetic standards. RLE-based compression technique proposed for volumetric image data is designed to be applied on 3D grey-scale image, which was produced by CT and homogeneous structure is not commonly applied. In another study [18], the authors characterized the textures of 3D-medical data into 26 variant displacements using means of the low computational-load and simply implemented RLE properties.

The file format of RLE algorithm can be implemented easily in real-time applications and embedded systems [19], [20]. In addition, it has the ability of volumetric data compression depending on the 3D predictors for utilizing correlation of inter-slices [4]. Berghom *et al.* [21] demonstrated the architectures of conditioning hybrid embedded coding that depends on context and RLE provided better performance regarding coding and execution time than other pure-entropy based coders. Such studies highlight the upcoming potential applications of RLE in field of image compression of binary medical data.

Up-to-date telemedicine protocols adopts standards of binary image compression like CALIC [9], JBIG [22], [23] and JBIG2 [24], quad-tree [25], and RLE [26]–[28], which are also adopted in other medical storage and archiving systems. In spite of considerable achievements and results of aforementioned techniques in binary data, they are not essentially designed to consider removing redundancies of binary images in medical data. Such that, significant redundant data is still exist and cannot be achieved using such standards. Besides, in the existing systems of medical image compression, only the correlations between intra-slice are utilized to handle the pixel redundancy [29]. On the other side, there are some disadvantages in volumetric methods considering their complexity regarding vector representation.

Such limitations provide considerable opportunities for potential contributions in binary compression of medical images. Consequently, despite the considerable compression ratios reached by industrial standards of image compression, there is chance to build compression algorithms to handle more redundancy of medical data. In such case, proposed techniques in compression standards recorded a weakness in the elimination of redundant parts, which is caused by the divergence of binary medical image from grey scale ones [1]. Due to the aforementioned, this paper proposes using 3D-run length encoding (3D-RLE) coding algorithm as a compression technique to transform image data into a transformed form of lower-entropy, where it scans organs morphology in the image considering. Proposed algorithm of this paper utilizes inter-slice correlations besides the ones of intra-slice, where low complexity of the algorithm and computational load are intended.

The contribution of the proposed method is illustrated in three parts in scope of lossless data compression of binary medical image. First part regards that proposed 3D-RLE is an adaptive form of 2D-run length encoding (2D-RLE) one, where it is designed such that it reveals medical data redundancy. It scans the



binary data coherently with organs shape. So far, for more redundancy found in the binary medical images, proposed technique is extended using five forms of scanning: perimeter (spiral), boustrophedonic, Hilbert (pi) and chevron, morton (quadrant) and additional parameters, which provide coherence with the procedure of scanning and the organs shape. Aldemir *et al.* [30] showed that such morphological coherence reduces the contribution of image entropy to the compression performance even though it utilizes correlations between intra-frame only. Providing such morphological coherence from the extension to various forms of scanning is applied by this paper in a volumetric form of RLE, which provides a considerable decrement in data entropy.

In the second part, combining intra-slice with inter-slice coding is utilized in this method to reveal the redundancy resulting by inter-slice correlations of voxel. Finally, third part contains the design in a parametric fashion to be suitable for telemedicine networks. Proposed algorithm of this method is applied on different datasets of medical image. The experimental results show the significant enhancement provided by the proposed algorithm against the existing standards of binary image.

The rest of this paper is organized to provide an overview of medical image compression and its application that adopted RLE coding technique next in section 2. The 3D form of RLE used in volumetric compression is illustrated thorough section 3. Section 4 discusses the experimental results yielded by the numerical simulations. Finally, section 5 provides the concluded remarks from results discussion.

## 2. RESEARCH METHOD

### 2.1. Using RLE technique in image compression

The simple/effective RLE is a coding algorithm widely adopted by lossless compression techniques. The principal concept in RLE method is to detect repetitions of image pixels through suitable scanning procedure in the image to be compressed. For clearer illustration of RLE concept, assume  $I: Z \times Z \rightarrow Z$ ,  $I(x, y) = l$  refers to a 2D image, in which  $i=1:M$ ,  $j=1:N$  represent spatial coordinates of each image  $(i, j)^{th}$  pixel,  $l \in [0, L-1]$  represent pixel intensities correspond the grey levels of the image and  $L=2^n-1$ ,  $n \in \mathbb{N}$  refers to the grey values within the range black level of grey (0) up to the white ( $L-1$ ). There are two major steps to build RLE coding algorithm, image mapping into a vector  $T: I(x, y) \rightarrow V$  using suitable searching technique like Linear, Perimeter or Boustrophedonic, and order. This defines the start and end positions of scanning technique and parameters where  $V = [Vk, k = 1, 2, \dots, (size) - 1, (size)]$ , ...  $size = M \times N$ . Second generates result RLE sequence of symbol pairs  $P = \{(vi, ri), i = 1, \dots, N\}$  utilizing  $R: Vk \rightarrow P$  transformation, where  $vi$  represents the value of the  $i$ th series of pixels with the same value repeated for  $ri$  times.

Next example illustrates aforementioned two steps, where Figure 1 contains an example of a mask of binary pixels as shown in Figure 1(a) which are scanned by Perimeter and Boustrophedonic searching technique [5]. The two searching techniques are represented using the two lines on the mask, which produces, for Boustrophe technique, V1 and V2 sequences as shown in Figure 1(b) and final P1 and P2 symbol pairs as shown in Figure 1(c). For perimeter technique, V1 and V2 sequences are presented in as shown in Figure 1(d) and final P1 and P2 symbol pairs are presented as shown in Figure 1(e). Obviously, two result pairs have different lengths and entropies since they are determined by coding and scanning procedures. Since the final value of compression ratio is affected by the entropy, optimizing these steps enhances compression performances of RLE-based techniques. All probabilities of RLE symbols  $P_i$  are also analyzed, since they, generally, satisfy the case of 2-k. In which, Huffman-coding is matched providing best code length [15].

Due to Figure 1, considering given sequence in the sample P1, corresponding probability of each symbol ( $s$ ) is defined as  $p(s) = (\text{symbol occurrence})/P$ . Such that, the probability values of such symbols in P1 are computed as  $p(0)=3/12$ ,  $p(1)=6/12$ , while  $p_3$ ,  $p_4$  and  $p_6$  have the same occurrence probability ( $1/12$ ), and hence, RLE symbols are handled through Huffman coding technique to build variable length coder (VLC) for producing code stream with optimal variable length. Since symbol sequences resulting from images of medical applications satisfy the negative power rule, this paper adopts Huffman coding technique for VLC.

Consequently, RLE approach reorders a matrix of image into low-entropy vector while revealing inter-pixels redundancy, which was adopted in 2D-space for mapping data into symbols by different state-of-the-art standards of compression [30]. RLE coding technique was previously used for binary and grey-scale image compression as entropy coding approach [4], [8], [31]. This paper adopts an inter-slice and parameterized version of RLE coding is designed for compression of 3D binary medical image. Proposed technique is designed in this paper regarding an integration of low-complexity, volumetric and parameterized approaches for a state-presentation of digital imaging and communications in medicine (DICOM). Following section discuss the details of the proposed algorithm.



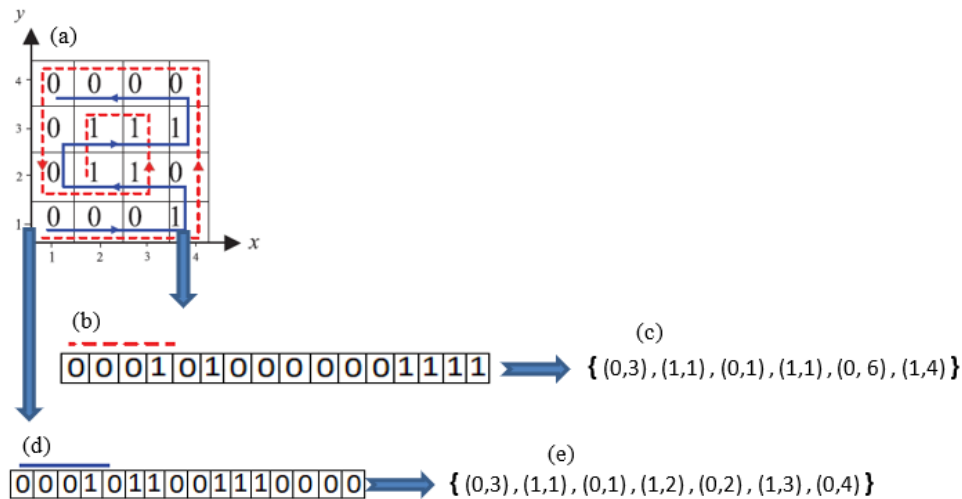


Figure 1. General concepts of RLE coding technique to show its simplicity and efficiency (a) original matrix, (b) boustroph searching result, (c) result boustroph bit stream, (d) perimeter searching result and (e) result perimeter bit stream

## 2.2. Lossless compression technique for volumetric data binary images

Although image compression techniques, that adopt 2D-RLE coding, combine efficiency and simplicity, only intra-slice correlations are utilized in such techniques. Besides they adopted only basic forms of scanning like linear and zigzag [1]. In previous RLE-based compression works, some disadvantages are carried out regarding computationally-complex representation [18]. As a result, this work adopts the 3D form of RLE for coding binary image:

- Due to the volumetric design and simple computations for lossless compression. This method has significant differences from the regular 2D-RLE compression techniques [2], where only intra-slice correlations are utilized [4], hence volumetric data compression is proposed by adopting correlations of inter-slice too. Furthermore, another extension is to employ multiple forms of scanning and order parameters for more compatibility scanning procedure and image organ. Thus, this can increase the efficiency of revealing the redundancy of inter-slice in binary medical images.
- Compression algorithm of this work is proposed to be a lossless technique, where resulting bit-stream of the compressed image is uniquely decodable (UD) without losing any detail or information. The proposed compression technique can be described using illustrated general block diagram in Figure 2, where it is divided into three main blocks matrix to stream scanning (volumetric), entropy coding RLE, and compression coding (Huffman). Next paragraphs discuss these blocks in detail. In the scanning block of the volumetric matrix, the aim is achieving a morphological coherence between the object shape and applied scanning procedure. The controlling factors of such procedure are its design in the volumetric approach, scanning order (O), slice depth (D) and scanning form (S), which are illustrated in the next paragraph. In other words, the image matrix is mapped into using a low-entropy representation of this vector. In the second block, RLE (R) converts resulting vector from previous step to a sequences of P symbols. Final Huffman block encodes the result symbol vectors  $\{P(n)\}$  into the final compressed bit-stream using VLC.

Three parameters specify the volumetric procedure of scanning, which are: i) scanner (S), represents selected technique for scanning on the specified route; ii) described order (O) by start and end locations of the matrix specified by the procedure; iii) depth (D) of the slice, which represents adjacent slices that are considered.

More illustration diagram about volumetric-RLE concepts is shown in Figure 3, which considers  $D=2$ ,  $S=4$  and  $O=3$  indicating start and end positions from  $(N, 1)$  to  $(N/2, M/2)$  respectively. Such parameters are assumed for an input matrix of image of  $M \times N \times K$  dimensions. Assume  $J3D[x, y, z]=1$  represents the raw 3D image matrix, where  $x, y$  represent spatial coordinates and  $z$  the  $\{0, 1\}$  pixel values for corresponding voxels. Figure 3(a) refers to the input image and matrix-to-vector mapping procedure is utilized for generating vector representation of each slice. Figure 3(b) illustrates the scanned sequences  $\{V_k, k=1, 2, 3, \dots, D\}$ , and the vectors  $V_1$  and  $V_2$ , which result from scanning corresponding first and the second slices. Then,  $V_1$  and  $V_2$  vectors are encoded into single  $V3D$  vector, which are in Figure 3(c). To define rule



generating of V3D, it compares the two vectors for elements with the same indexes. Pixels with same values keep it as it is, pixels with different values are encoded by adding ( $h_i$ ), where  $i=1, 2, \dots, M \times N$  prefix header for decoding ciphered values. The proposed algorithm is illustrated in Table 1.

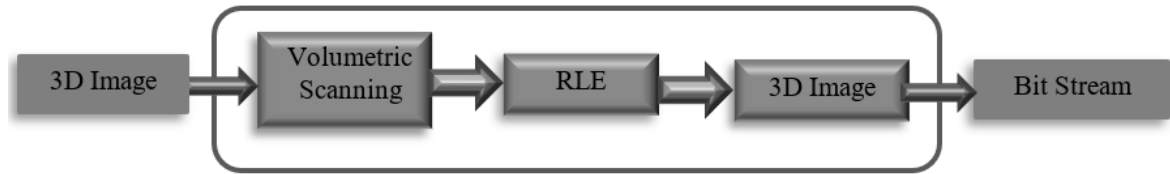


Figure 2. General diagram of the proposed compression technique including general blocks

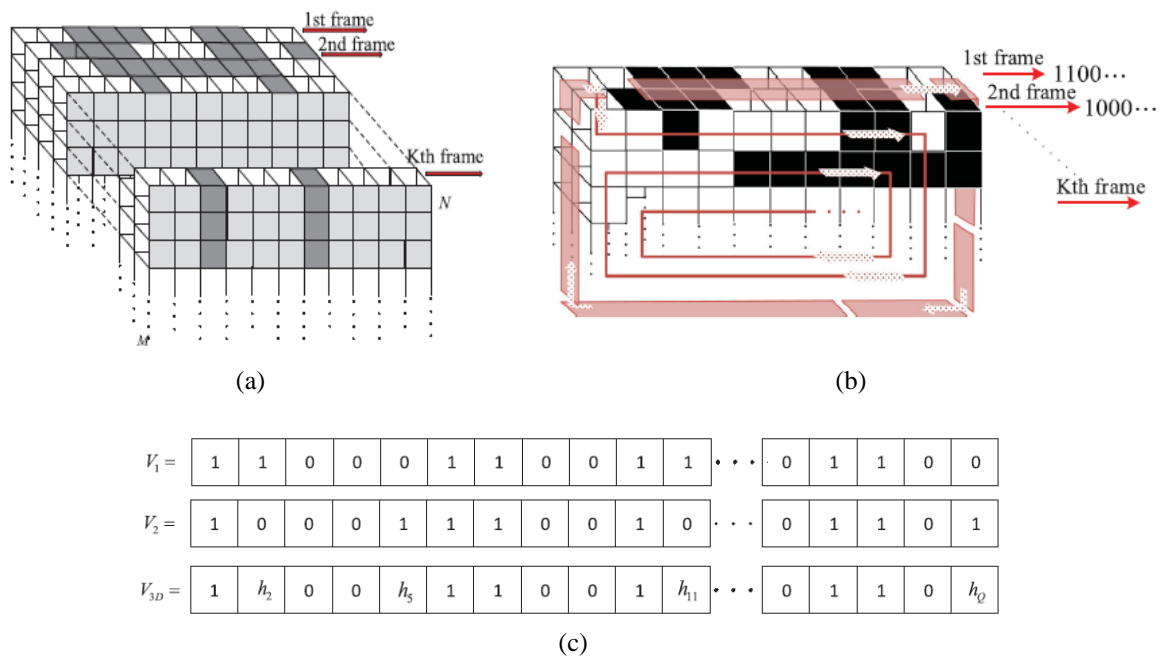


Figure 3. Adopted procedure in volumetric scanning of image matrix where slice depth=2 (a) input 3D image, (b) perimeter scanning with D=2, and (c) result vector considering D=2

A principal motivation of this algorithm bases on same pixel value assigned to the pixels and the voxels, which indicates high correlation between slices. Accordingly, multiple ( $V_k$ ) vectors can be encoded into a single ( $V_{3D}$ ) vector, which requires minimum possible prefix codes ( $h$ ). In such case, scanning procedure provides sequences with low entropies  $V_k$ , where higher prefix umbers decrease the performance of compression method. Given pseudo code in Table 1 provides the ability of compressing the input images using (2D or 3D) RLE coding utilizing parameters of the scanning. Ordinary 2D-RLE extends the encoding procedure to multiple forms of scanning, where it is applied on each slice regardless the correlations inter-slice (Table 1-A). Unlikely, 3D-RLE utilizes intra-slice correlations in addition to inter-slice ones using volumetric scanning facility (Table 1-B). First part includes mapping image slices into ( $V$ ) vector, where  $V=\{V_k=T(I_k), \forall I_k [J3D], k=1, 2, \dots, K\}$  using  $T: Z \times Z \rightarrow Z$  transformation. This is controlled by (S) form and (O) order where  $I_k$  represents  $k^{\text{th}}$  slice of J3D (Table 1-A-1). Next step include applying the mapping function ( $R: Z \rightarrow Z$ ) of RLE to each  $V_n$  for constructing  $\{P, P_k=R(V_k), \forall V_k \in V, k=1, 2, \dots, K\}$  (Table 1-A-2). The next step, Huffman coding technique is used to convert sequence symbols  $P_k$  into bit-stream  $C_k$  (Table 1-A-3), and therefore all result slices from RLE are encoded compressed into bit-streams. Transformation of RLE, which is as same as operations discussed in previous sections, provides ( $v, r$ ) pairs of symbol. In such symbols, values of successive pixels, of  $V_n$  sequence, are the same, where  $rm$  represents the number of successive similar pixel values.



In Table 1-B, D is set to be greater than (1) to represent utilizing inter-slice correlations and intra-slice ones in image are compression. Slice scanning is accomplished by T to assign the output sequences into M3D row (Table 1-B-6). Then over M3D columns, non-overlapping blocks and (D) depth, if voxel values are different in the block, then to satisfy uniquely decodable (UD) property, the prefix h (1) is computed and the output is encoded into V3D (Table 1-B-9). Then, bias value is set to 1 to avoid having 0 and 1 values for h, else this conflicts the case of having same values for block voxels (0 and 1), which are encoded as 0 and 1 (Table 1-B-8), respectively. Sections 8, 10 and 12 of Table 1-B performs append operation, e. g., where  $i_1=i_2=1$ ,  $D=3$ ,  $M3D [1: 3, 1]=[1 \ 0 \ 0]$ , and h header provides 1. This is not considered as uniquely decodable case, one-to-one mapping, whereas they are the same satisfying M3D condition (all-equal). As a result, adding bias=1 to h makes the code fulfill UD property. The code is also satisfying UD property for all values of slice-depth and conditions.

$$h = 1 + \sum_{k=0}^{D-1} 2^k M_{3D}[i_1 + k, i_2] \quad (1)$$

Table 1. Illustrating the pseudo code of the proposed 3D RLE coding algorithm

INPUTS:	3D image, scanning form, order, and slice-depth
Raw Image :	$J_{3D} = \{I_k \in Z \times Z \text{ where } k = 1, 2, \dots, K\}$ and $k \in Z^+$ represent slice number in the input image
Scanning Form (S):	$S = \{\text{Linear, Boustrophedonic, Zigzag, Perimeter, Morton, Hilbert and Chevron}\}$
Scanning Order (O):	$O = \{(+x, +y), (+y, +x), (+x, -y), (-x, -y), (-y, -x), (-y, +x), (+y, -x)\}$
Slice Depth :	$\forall D \in Z^+ \text{ and } D \leq K$
Initialization	$i = 1, i_0 = 1, Q = M \times N, i_1 = 1, i_2 = 1$
(A)	<p>if <math>D = 1</math> then , Encode each slice individually, (intra-slice correlations only).</p> <p>while <math>i &lt; k</math>, Do Convert the matrix to a vector base on S &amp; O parameters.</p> <ol style="list-style-type: none"> <li>For each slice, construct re-ordered vector for the ith slice <math>V_i[k] \in Z, k = \{1, 2, \dots, Q\}</math> by transforming the input image (li) into the vector (Vi) using scan result of ith slices <math>I_i \in J_{3D}</math> regarding S and O parameters .</li> <li>Apply RLE procedure to convert Vi to the symbol vector (Pi) with (v, r) pairs.</li> <li>Apply Huffman entropy coding technique to convert Symbol vector (Pi) to final bit-stream (c)</li> <li>Save C results and increase <math>i \rightarrow i+1</math> and iterate the operation on next slice.</li> <li>Accumulate each result C to construct the final bit-stream C3D.</li> </ol> <p>if <math>D &gt; 1</math> then;</p> <p>Utilize inter-slice correlations with intra-slice with ones to compress J3D image.</p> <p>while <math>i_0 = K</math> Do convert <math>i_{10}</math> to <math>V_{i0}</math> based on S &amp; O parameters</p> <ol style="list-style-type: none"> <li>Construct the M3D matrix, where each sequence <math>V_{i0}</math> is related with its corresponding <math>i_{10}</math>th row in the matrix M3D.</li> <li>Increase the counter by one (<math>i_0 = i_0 + 1</math>) to handle the next slice.</li> </ol> <p>while <math>i_2 \leq K</math>, Do</p> <p>while <math>i_1 \leq Q</math>, Do</p> <p>if <math>M_{3D} = [i_1, i_2] = M_{3D} = [i_1 + 1, i_2] = \dots = M_{3D} = [i_1 + D, i_2]</math>, then</p> <ol style="list-style-type: none"> <li>Accumulate V3D by <math>M3D[i_1, i_2]</math></li> </ol> <p>ELSE</p> <ol style="list-style-type: none"> <li><math>h_{i1} = 1 + \sum_{j=1}^{D-1} 2^j M_{3D}[i_1 + j, i_2]</math></li> <li>Accumulate V3D by <math>h_{i1}</math></li> <li>Increase <math>i_1</math> by 1 (<math>i_1 = i_1 + 1</math>)</li> <li>Add the escape character 'ch' to recognize groups of constructive slices:</li> </ol> <p>Accumulate V3D by 'ch'</p> <ol style="list-style-type: none"> <li>Add D to <math>i_2</math> (<math>i_2 = i_2 + D</math>)</li> <li>Apply RLE to construct sequence of symbol (P3D)</li> <li>Get C3D bit-stream using entropy encoder for P3D sequence.</li> <li>Save the compressed bitstream (C3D).</li> </ol>
(B)	Encoded/compressed bit-stream (C3D)

As aforementioned, scanning procedure has three parameters, scanning order (O), scanning form (S), and slice-depth (D), they have significant effects on the efficiency of compression technique, where sequences with low entropy can be only achieved when appropriate O, S, and D are determined. In an image with  $M \times N$  resolution, each scanning form has 4 scanning orders to indicate indexes of start and end positions regarding the adopted scanning procedure. The seven scanning forms and their orders are illustrated in Table 2. For boustrophedonic and Hilbert forms, (x, y), (y, x), (x, -y) and (-x, -y) orders are illustrated in Figures 4(a) to 4(d) respectively. Directing arrows are used to figure out scanning procedures considering specified scanning form and order. For (Morton) scanning form, (1, 1) and (N, M) and (+y, +x) are assumed to represent start, end and order indexes respectively, and remaining scanning forms are illustrated in Figures 5(a) linear, 5(b) boustrophedonic, 5(c) zigzag, 5(d) perimeter, 5(e) morton, 5(f) Hilbert, and 5(g) chevron. Selecting multiple scanning forms and orders provides morphological coherence between organ shape and scanning forms, which decreases data-sequence entropy leading to higher compression performance.



Table 2. Scanning orders (O) for scanning techniques

Scanning Form		Directions				
		+x, +y	+y, +x	+x, -y	-x, -y	-y, -x
Linear	Start	(1, 1)	(1, 1)	(N, 1)	(N, M)	-
	End	(N, M)	(N, M)	(1, M)	(1, 1)	-
Boustrophedonic	Start	(1, 1)	(1, 1)	(N, 1)	-	(N, M)
	End	(N, 1)	(1, M)	(1, 1)	-	(N, 1)
Zigzag	Start	(1, 1)	(1, 1)	(N, 1)	(N, M)	-
	End	(N, M)	(N, M)	(1, M)	(1, 1)	-
Morton	Start	(1, 1)	(1, 1)	(N, 1)	-	(N, M)
	End	(N, M)	(N, M)	(1, M)	-	(1, 1)
Perimeter	Start	(1, 1)	-	(N, 1)	(N/2, M/2)	(N/2, M/2)
	End	(N/2, M/2)	-	(M/2, N/2)	(M, N)	(N, 1)
Hilbert	Start	(1, 1)	(1, 1)	(N, 1)	-	-
	End	(N, 1)	(1, M)	(1, 1)	-	-
Chevron	Start	(1, 1)	(1, 1)	(N, 1)	(N, M)	-
	End	(N, 1)	(1, M)	(1, 1)	(N, 1)	-

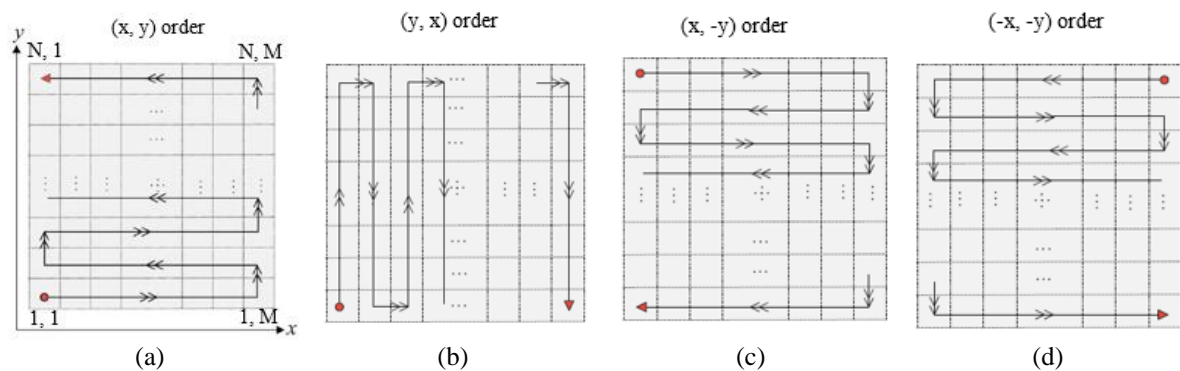


Figure 4. Scanning directions and their effects on the output start and end of scanning procedure in boustrophedonic technique (a) x, y order, (b) y, x order, (c) x, -y order, and (d) -x, -y order

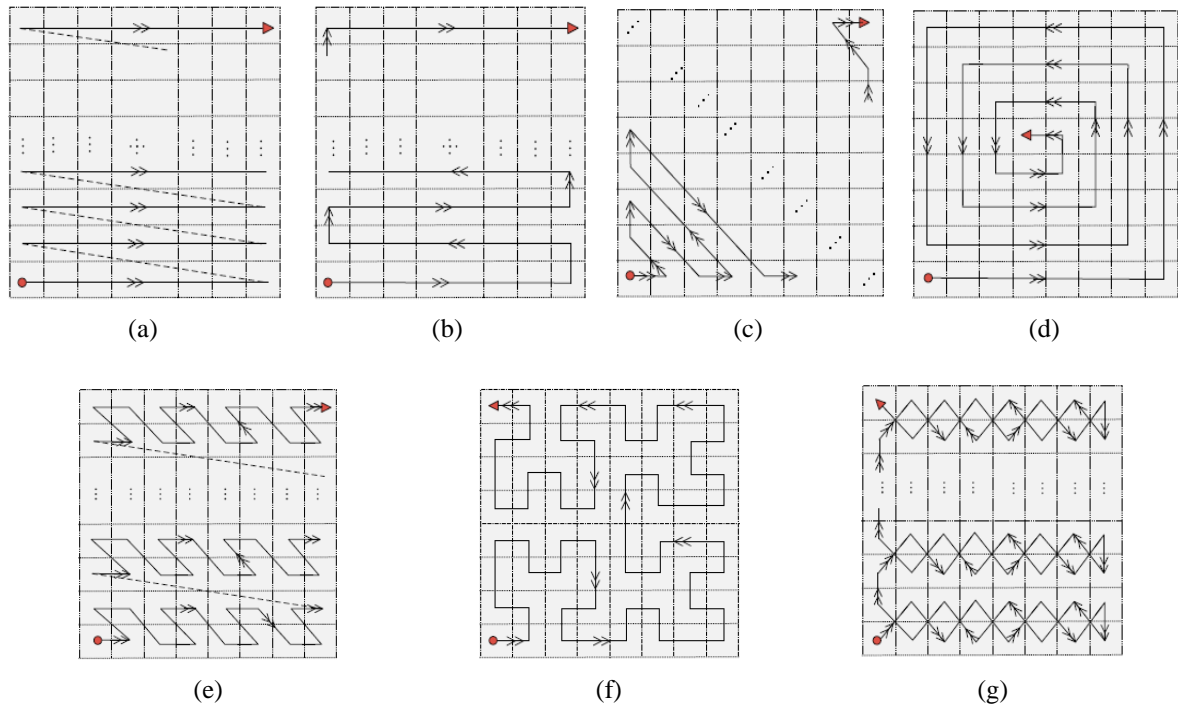


Figure 5. The general tracking system due to the seven scanning techniques (a) linear, (b) boustrophedonic, (c) zigzag, (d) primeter, (e) morton, (f) Hilbert, and (g) chevron



Whereas, such technique is also executed using the volumetric form in order to attain the neglected potentials of arising redundancy because of inter-slice correlation. Consequently, the effect of scanning procedure on the performance of proposed compression algorithm is significant. The pipeline of 3D-RLE differs from 2D-RLE techniques where only intra-slice correlations are utilized to scan the matrix seeking for low-computational task. While, in this case (volumetric direction), both intra-slice and inter-slice correlations must be utilized. Besides, proposed method utilizes extra of forms scanning for morphological coherency with the segmented organ in the medical image. This illustrates the evident that adjacent pixels are directly correlated to the voxels of binary images. Additionally, correlated elements of an image represent a major source to code image redundancy. Due to the aforementioned information, 3D-RLE approach attains considerable compression ratios (CR), whereas it considers the medical architecture of binary images. Experiments of proposed compression technique were conducted on different types of medical image, one CT, two MR) and private datasets. MRI datasets are sub-divided into MR-T1 dual and spectral pre-saturation with inversion recovery (SPIR) sequences.

### 3. RESULTS AND DISCUSSION

The proposed compression technique using 3D-RLE illustrated pipeline is applied on aforementioned datasets, which are in details: i) abdominal CT, ii) abdominal MR-T2 (SPIR) sequence, iii) abdominal MR-T1 dual sequence, and iv) uniformly distributed random image datasets. The first dataset CT contains different sets of slices for 20 patients, which vary from 77 (min) and 105 (max) slices per 3D-image for each patients (90 slices on average), with up to 1992 slices in total. This paper studies 3D-binary image for different patients and each of them has attributes such as: (512×512) resolutions, x–y spacing from 0.7-0.8 mm and 3-3.22 mm for inter-slice distance (ISD). Each of the two MRI (T1 and T2) datasets contains medical images for 20 patients with (40) images as total number. Both of them consist of 3D binary images of segmented liver with (256×256) resolutions, (1.36-1.89) mm x–y spacing, and 5.5-9 mm for ISD. Both (T1 and T2) MRI datasets contains between 26 and 50 slices (average 30 slices) for dataset images, and their totals are (625 and 612) images. All dataset contains binary images of segmented liver [32]. The private dataset contains 20 volumetric images, which are as same specifications as CT dataset for a quantitative comparison of the performance. However, it has no spatial or temporal voxel-correlations. Experimental evaluations are performed using the CR. Figures 6(a), 6(b), and 6(c) shows examples of grey scale image of International Council Of Museums Converter Computed Tomography (ICOM CT), segmented binary image of CT, and uniformly-distributed 3D-image random of distributed values respectively.

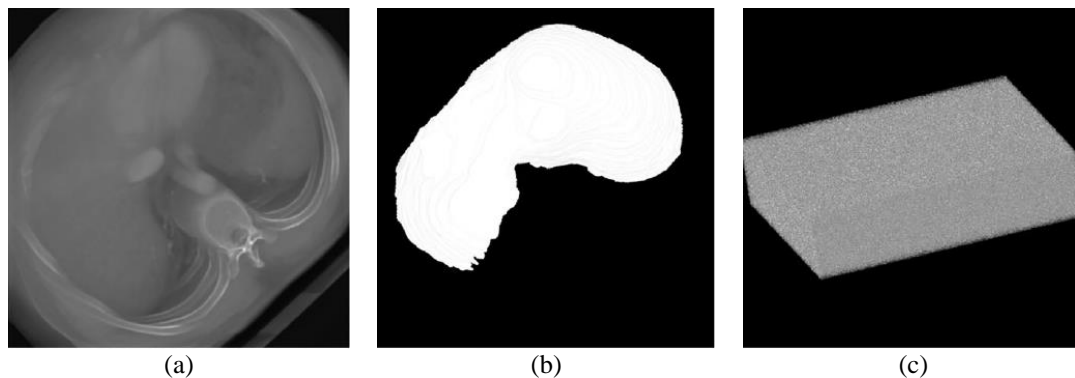


Figure 6. These figure are samples of (a) grey scale image of ICOM CT, (b) segmented binary image of CT, and (c) randomly distributed 3D-image

The 3D-RLE algorithm is adopted to compress dataset images due the same illustrated diagram in Figure 2, which is as same as 2D-RLE without utilizing correlations of inter-slices. Both (2D and 3D) RLE algorithms adopt aforementioned forms of scanning besides the widely adopted forms (zigzag and linear). For a comparison with 3D-RLE, 2D-RLE procedure is also applied on dataset images, which previously applied in another study [33] with extended scanning form to attain a rigid CR since inter-slice correlations were not utilized. Yielded results are benchmarked with other standards of lossless compression applied on binary images like JPEG2000, PNG, CCITT-G4, JXR, and ZIP, LZW, JBIG and JBIG2.



Adopting CT dataset, Figure 7 demonstrate the performances of all compression methods on the studied dataset, where 3D-RLE attained 1:115 against 1:112 CR value for robust standard compressor (JBIG2). Other standards of compression attained less than 1:100 ratios. The remaining parameters of 3D-RLE compression scheme were (6, 3, and 4) for Hilbert scanning, scanning order, and slice depth respectively. Ordinary 2D-RLE was also applied using same other scanning parameters, where D=1 to indicate utilizing intra-slice correlations only. A conclusion is drawn about the redundancy of coding between image slices, which contributes compression efficiency.

On the other side, proposed compression scheme in this work yielded better results than other state-of-the-art successful compression procedures like JBIG2. Proposed method was applied on MRI images, with slices that have more ISD than CT images. Figure 8 illustrates the average of results yielded by simulation applied on weighted images from (MR-T1 and MR-T2). Parameter values adopted in 3D-RLE experiments of this comparison were (s=6, O=3, and D=3) for Hilbert scanning, scanning order, and slice depth respectively, while 2D-RLE was also applied using same parameters except D=1 for slice depth. As similar to CT comparison, the proposed compression scheme attained up to 1:90 for CR value which overcomes other state-of-the-art ratios on MRI datasets. Yet, the performance of proposed compression scheme as same as other methods was generally decreased. After the proposed technique, JBIG2 and JBIG yielded the best performance among the remaining methods, where they yielded less than (1:30) and some of them yielded half of their performance in CT comparison. Despite the satisfactory enhancement in CR values of CCITT-G4 and JPEG-2,000 on CT dataset, their CR values on MR dataset still around (1:20) value for CR. Such ratio represents a weak performance among other values on MR datasets. Generally, regarding that the decrement in ISD value increases slice-correlations, method performance on CT dataset is higher than its performance on MR dataset. This illustrates that inter redundancy of voxel reveals higher efficiency in CT dataset than in MR dataset. The ISD represents a principal effect behind such result, where it determines correlation levels of inter-slices. Better performance attainable by adopting specific system of image acquisition to provide image with lower level of ISD. This indicates the obvious effects of ISD on method performance, where better performance can be attained. Proposed method has a parameterized design to reveal maximum possible redundancy.

Another direct-effect parameter is the order, which has obvious effects on method performance. Dataset images are compressed utilizing all scanning orders as shown in Table 2, where, as example in Hilbert scanning form, order 2 starts from (1, 1) and ends to (1, M). General performance attained by 3D-RLE on CT dataset is illustrated in Figure 9 regarding compression parameters (S, O, and D=4), while Figure 10 demonstrates general attained performance on MRI dataset (average of MR-T1 and MR-T2). The considerable result to be discussed is that high value of CR was achieved by Perimeter, Morton and Hilbert scanning forms over most cases on CT and MRI datasets. In the case of order-3 of scanning, most of compression parameters attain best values of CR, which also indicate that adopted scanning forms have the minimum dependency with the parameters of order. On the other hand, other scanning forms like Linear and Z had fluctual performance due to their orders. Zigzag scanning form was widely adopted in industrial standards of compression that adopt transformations, in which group its coefficients together as small to large frequencies for significant results in coefficient-seeking stage of the transform. However, CR value yielded by linear, zigzag and chevron is relatively low using 3D-RLE approach. Another remark can be concluded from Figures 9 and 10 whereas Hilbert, morton and perimeter have more result-significance than other forms of scanning.

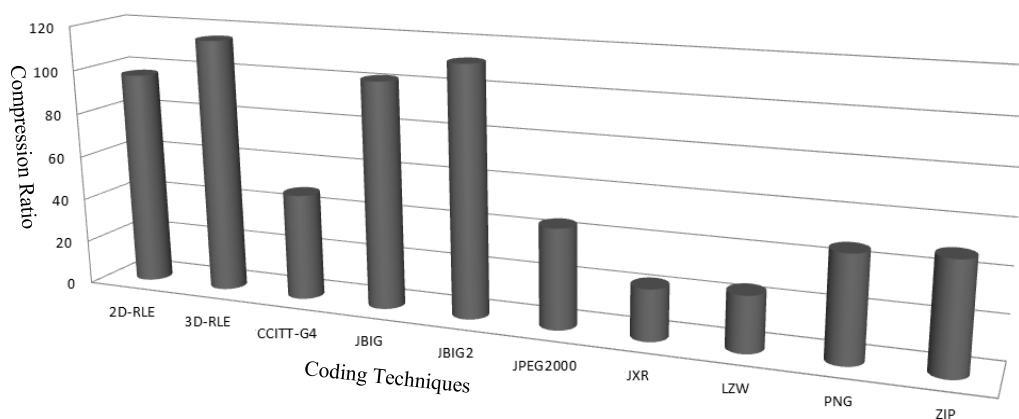


Figure 7. General performance as a result from applying different compression techniques on CT images



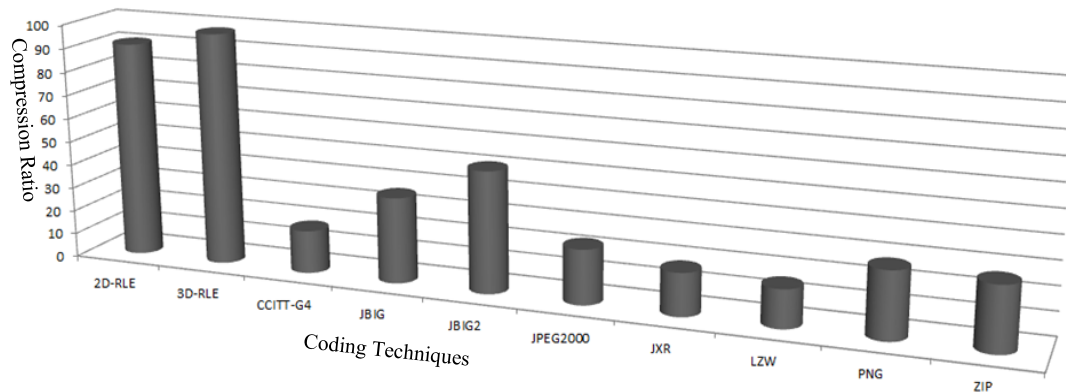


Figure 8. General performance as a result from applying different compression techniques on MRI images

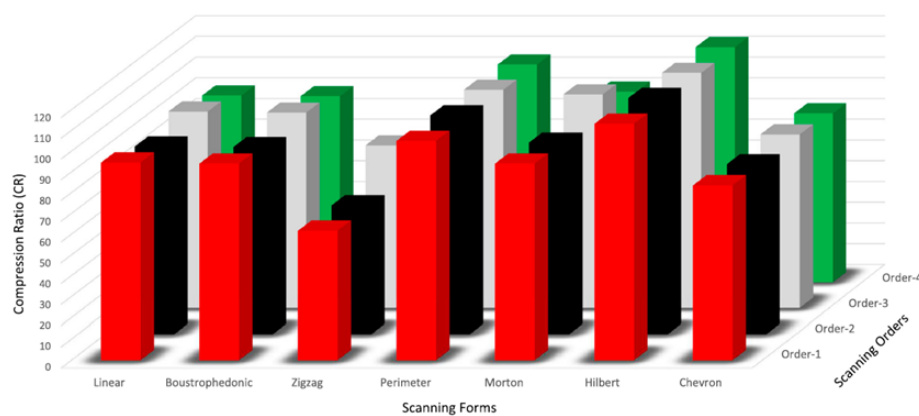


Figure 9. 3D-RLE performance on CT dataset using all forms and orders of scanning, when D=4

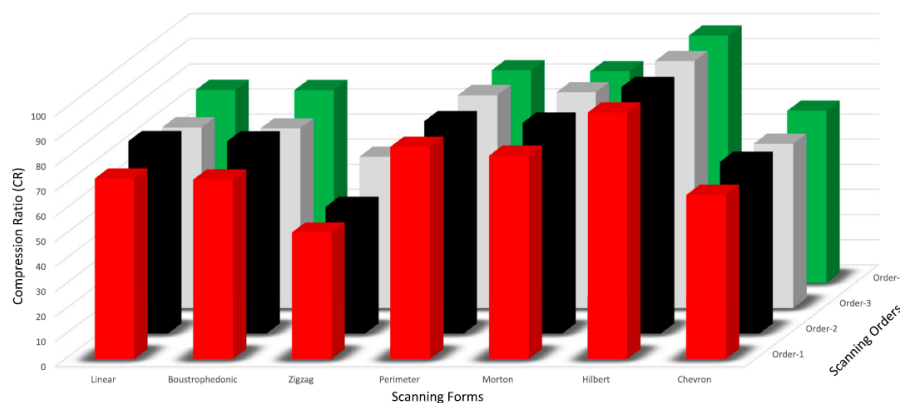


Figure 10. 3D-RLE performance on MRI dataset using all forms and orders of scanning, when D=3

Where tuning compression parameters achieves best possible morphological coherence, organ shape should be considered in the segmented image, i.e., oval-shape organs having yields better CR values using Perimeter scanning. Accordingly, such parameters should be tuned considering image to be compressed. Private-dataset compression is accomplished using both 2D-RLE, 3D-RLE, which benchmarked with state-of-the-art techniques. Since such dataset, as compared MRI and CT datasets, has no correlations for intra-slice and inter-slice, only weak redundancy amount can be revealed either using proposed compression scheme or other compression standards. Yielded CR values by all techniques are smaller than 1 providing



negative compression on such dataset. As example, where CR is equal to (0.086, 0.12 and 0.074) for 3D-RLE, PNG, and JPEG2000 respectively, yielded CR by scanning forms are instable, and optimal set of parameter are indeterminable for such dataset.

Experiments of this work are conducted using a range of slice depth  $\{D, D \in [1, 11]\}$ , which determines best possible value for  $D$  in 3D-scanning. Attained performances 3D-RLE approach depends on  $D$  dependency to compress MR-T1, MR-T2 and CT datasets. Experiments were conducted on images for 20 patients, and the average value of them are illustrated in Figure 11 considering  $S=4$ , scanning forms (Perimeter) under average of results for applying 4 orders (O). Results showed that ( $D=4$  or 5) values yielded best CR regarding CT dataset where average ISD=3 mm. While for MRI datasets, best CR value is attained with slice depth ( $D=3$  or 4), where MRI's ISD has relatively higher values. The concluded remark from such results indicates the higher correlation between slices in CT images than in MR images. Obviously, the approach with higher correlations between inter-slices attains higher CR value indicating better compression performance whereas selected slice depth is optimal. This highlights the dependence between the distance of 3D image's inter-slice and the number of correlated slices. Accordingly, proposed compression technique achieves better performance handling CT dataset than with MRI dataset. In addition, CT images have higher correlations between inter-slices than with MR images.

Consequently, 3D-RLE concept considers reordered sequences with low-entropy located in the raw data. Images are mapped using specific scanning procedure, which is specified by its parameters, where a morphological coherence is attained between scanning procedure and organ shape. Such parameters have preliminary effects on algorithm performance. A conclusion from experimental results, determining the proper parameters of form, order and slice-depth is a contribution to the method performance on correlated data in the medical images. This can be achieved where organs shape is considered as the key point to enhance CR value. At same context, Morton, Perimeter, and Hilbert provide considerable performances independently from the scanning order. Yet, the redundancy is not effectively revealed for uncorrelated data. Where liver and scanning form have morphological compatibilities in all of datasets, the highest amount of voxels, in series is caught. This can be considered as optimum for 3D-RLE proposed in this algorithm.

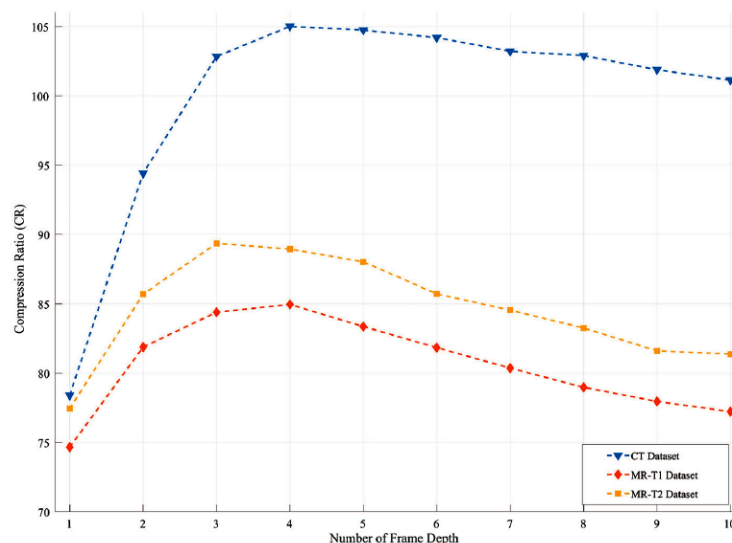


Figure 11. 3D-RLE performance on all datasets CT, MR-T1, and MR-T2 regarding different values of depth ( $D=1, 2, 10$ )

#### 4. CONCLUSION

In this paper, RLE is presented regarding 3D case to be applied in compressing binary medical images under the name 3D-RLE. It is proposed in a volumetric and parameterized form to improve CR value and compression performance. A morphological coherence is provided between object shapes and adopted scanning procedure, where less image entropy constructs the major concept of this study. Using the scanning procedure, proposed technique characterizes 3D images by mapping voxel values depending on  $S$ ,  $O$ , and  $D$  parameters. The main task is achieving as low-entropy as possible vector of sequences that corresponds the images. The proposed compression technique combines inter-slice with intra-slice correlations to apply RLE



approach for revealing encoded redundancy between image values. Thus, high CR values are provided by the significant entropy decrement.

A numerical simulation is applied on several datasets of medical images (volumetric CT and MRI). A conclusion is extracted from the results that object-shapes and scanning procedure have morphological coherence, which is restricted by scanning parameters. In other words, organ shape has direct effects on the efficiency of compression performance. Achieved coherence using a proper scanning procedure decreases image entropy by mapping an image matrix into a form, where voxel intensities have fewer transitions. Adopted algorithm in this work is totally parameterized in order to optimize the form (and/or order) of the scanning, where decreasing image entropy provides best possible CR values. Perimeter, Hilbert and Morton forms of scanning achieved higher CR values than the other forms. Besides, varying scanning orders adopted by these forms yielded insignificant differences in their performances. This indicates that such forms have less dependency on scanning order than other ones. Benchmarking with state-of-the-art standards, experimental results yielded considerable progression regarding compression efficiency. Optimal D value represents another conclusive parameter that affects system performance. Selecting optimal value for D is directly affected by distances between inter-slices in volumetric images. Where wider distances indicate weaker correlations, selected D values must consider higher distances in volumetric images. According to the observations, optimal D value for MRI dataset is smaller than the one for CT dataset. Accordingly, considering D value is crucial for effectively redundant removal from data. On the other side, proposed technique has more efficient ability of removing data redundancy than exploiting intra-slice correlations only.

Due to the low complexity of computations in 3D-RLE algorithm and its easiness of implementation, proposed compression technique can be significantly adopted by telemedicine applications. This is because it can efficiently compress and exchange binary medical images. In addition, the proposed method is recommended to be examined on other types of dataset like PET imaging, where they for their optimal numbers of D values, different inter-slice distances and same modalities used for image acquiring with different distances.

## ACKNOWLEDGEMENTS

The first author would like to thank Middle Technical University ([www.mtu.edu.iq](http://www.mtu.edu.iq)) Baghdad, Iraq for it is support in the present work. The second author would like to thank Mustansiriya University ([www.uomustansiriyah.edu.iq](http://www.uomustansiriyah.edu.iq)) Baghdad, Iraq for it is support in the present work.

## REFERENCES




- [1] M. Zarei, A. Rezai, and S. S. Falahieh Hamidpour, "Breast cancer segmentation based on modified Gaussian mean shift algorithm for infrared thermal images," *Computer Methods in Biomechanics and Biomedical Engineering: Imaging and Visualization*, vol. 9, no. 6, pp. 574–580, 2021, doi: 10.1080/21681163.2021.1897884.
- [2] J. M. Dahiru, "Knowledge and utilization of health informatics among medical doctors in Ahmadu Bello University Teaching Hospital, ShikaZaria," *International Journal of Informatics and Communication Technology*, vol. 10, no. 3, pp. 171–181, 2019, doi: 10.11591/ijict.v10i3.pp171-181.
- [3] R. S. Barros *et al.*, "Dynamic CT perfusion image data compression for efficient parallel processing," *Medical and Biological Engineering and Computing*, vol. 54, no. 2–3, pp. 463–473, 2016, doi: 10.1007/s11517-015-1331-6.
- [4] L. F. R. Lucas, N. M. M. Rodrigues, L. A. Da Silva Cruz, and S. M. M. De Faria, "Lossless compression of medical images using 3-D predictors," *IEEE Transactions on Medical Imaging*, vol. 36, no. 11, pp. 2250–2260, 2017, doi: 10.1109/TMI.2017.2714640.
- [5] I. Q. Abduljaleel and A. H. Khaleel, "Significant medical image compression techniques: a review," *TELKOMNIKA (Telecommunication Computing Electronics and Control)*, vol. 19, no. 5, pp. 1612–1621, Oct. 2021, doi: 10.12928/telkomnika.v19i5.18767.
- [6] F. Fischer, M. A. Selver, O. Dicle, and W. Hillen, "Performance comparison of compression algorithms for archiving segmented volumetric binary medical data," *Studies in Health Technology and Informatics*, vol. 205, pp. 1138–1142, 2014, doi: 10.3233/978-1-61499-432-9-1138.
- [7] M. W. Hoffman, "Lossless bilevel image compression," *Lossless Compression Handbook*. Elsevier, pp. 327–349, 2003, doi: 10.1016/B978-012620861-0/50018-8.
- [8] Y. T. Chen and D. C. Tseng, "Wavelet-based medical image compression with adaptive prediction," *Computerized Medical Imaging and Graphics*, vol. 31, no. 1, pp. 1–8, 2007, doi: 10.1016/j.compmedimag.2006.08.003.
- [9] E. Ageenko and P. Fränti, "Lossless compression of large binary images in digital spatial libraries," *Computers & Graphics*, vol. 24, no. 1, pp. 91–98, Feb. 2000, doi: 10.1016/S0097-8493(99)00140-5.
- [10] R. S. M. Wrembel, "RLH: bitmap compression technique based on run-length and Huffman encoding," *Information Systems*, vol. 34, no. 4–5, pp. 400–414, 2009, doi: 10.1016/j.is.2008.11.002.
- [11] B. Strasser, A. Botea, and D. Harabor, "Compressing optimal paths with run length encoding," *Journal of Artificial Intelligence Research*, vol. 54, pp. 593–629, Dec. 2015, doi: 10.1613/jair.4931.
- [12] A. Bovik, *Handbook of image and video processing*. Academic Press, 2005.
- [13] Y. Shan, Y. Ren, G. Zhen, and K. Wang, "An enhanced run-length encoding compression method for telemetry data," *Metrology and Measurement Systems*, vol. 24, no. 3, pp. 551–562, 2017, doi: 10.1515/mms-2017-0039.
- [14] M. M. Galloway, "Texture analysis using gray level run lengths," *Computer Graphics and Image Processing*, vol. 4, no. 2, pp. 172–179, 1975, doi: 10.1016/s0146-664x(75)80008-6.






- [15] C. S. Kim and C. C. J. Kuo, *Data compression*, 5th ed., vol. 1. Springer, 2011.
- [16] E.-H. Yang and L. Wang, "Joint optimization of run-length coding, Huffman coding, and quantization table with complete baseline JPEG decoder compatibility," *IEEE Transactions on Image Processing*, vol. 18, no. 1, pp. 63–74, Jan. 2009, doi: 10.1109/TIP.2008.2007609.
- [17] A. L. Liaghati and W. D. Pan, "Evaluation of the biased run-length coding method on binary images generated by a modified ising model," in *SoutheastCon 2016*, Mar. 2016, pp. 1–8, doi: 10.1109/SECON.2016.7506658.
- [18] D. H. Xu, A. S. Kurani, J. D. Furst, and D. S. Raicu, "Run-length encoding for volumetric texture," *Proceedings of the Fourth IASTED International Conference on Visualization, Imaging, and Image Processing*, vol. 27, no. 25, pp. 534–539, 2004.
- [19] B. Stankic, D. Kojic, M. Cvetanovic, M. Dukic, S. Stojanovic, and Z. Radivojevic, "ERLE: embedded run length image encoding," in *2014 22nd Telecommunications Forum Telfor (TELFOR)*, Nov. 2014, pp. 975–978, doi: 10.1109/TELFOR.2014.7034569.
- [20] C. H. Messom, G. Sen Gupta, and S. N. Demidenko, "Hough transform run length encoding for real-time image processing," *IEEE Transactions on Instrumentation and Measurement*, vol. 56, no. 3, pp. 962–967, Jun. 2007, doi: 10.1109/TIM.2006.887687.
- [21] W. Berghom, T. Boskamp, M. Lang, and H. O. Peitgen, "Context conditioning and run-length coding for hybrid, embedded progressive image coding," *IEEE Transactions on Image Processing*, vol. 10, no. 12, pp. 1791–1800, Dec. 2001, doi: 10.1109/83.974564.
- [22] D. Špelič and B. Žalik, "Lossless compression of threshold-segmented medical images," *Journal of Medical Systems*, vol. 36, no. 4, pp. 2349–2357, 2012, doi: 10.1007/s10916-011-9702-5.
- [23] L. Shen and R. M. Rangayyan, "A segmentation-based lossless image coding method for high-resolution medical image compression," *IEEE Transactions on Medical Imaging*, vol. 16, no. 3, pp. 301–307, Jun. 1997, doi: 10.1109/42.585764.
- [24] Ó. J. Rubio, Á. Alesanco, and J. Garcia, "Introducing keytagging, a novel technique for the protection of medical image-based tests," *Journal of Biomedical Informatics*, vol. 56, pp. 8–29, Aug. 2015, doi: 10.1016/j.jbi.2015.05.002.
- [25] H. Jiang, Z. Ma, Y. Hu, B. Yang, and L. Zhang, "Medical image compression based on vector quantization with variable block sizes in wavelet domain," *Computational Intelligence and Neuroscience*, vol. 2012, pp. 1–8, 2012, doi: 10.1155/2012/541890.
- [26] R. Shyam Sunder, C. Eswaran, and N. Sriraam, "Medical image compression using 3-D Hartley transform," *Computers in Biology and Medicine*, vol. 36, no. 9, pp. 958–973, Sep. 2006, doi: 10.1016/j.compbiomed.2005.04.005.
- [27] X. Qi and J. Tyler, "A progressive transmission capable diagnostically lossless compression scheme for 3D medical image sets," *Information Sciences*, vol. 175, no. 3, pp. 217–243, Oct. 2005, doi: 10.1016/j.ins.2005.01.008.
- [28] D. A. Koff and H. Shulman, "An overview of digital compression of medical images: Can we use lossy image compression in radiology?," *Canadian Association of Radiologists Journal*, vol. 57, no. 4, pp. 211–217, 2006.
- [29] S. Mantaci, A. Restivo, G. Rosone, and M. Sciortino, "Burrows-wheeler transform and run-length encoding," *Lecture Notes in Computer Science (including subseries Lecture Notes in Artificial Intelligence and Lecture Notes in Bioinformatics)*, vol. 10432, pp. 228–239, 2017, doi: 10.1007/978-3-319-66396-8\_21.
- [30] E. Aldemir, G. Tohumoglu, O. Dicle, and M. A. Selver, "Lossless compression of segmented 3D binary data for efficient telemedicine applications," in *104th Radiological Society of North America 2018 Scientific Assembly and Annual Meeting*, 2018, pp. 25–30.
- [31] S. Anantha Babu, P. Eswaran, and C. Senthil Kumar, "Lossless compression algorithm using improved RLC for grayscale image," *Arabian Journal for Science and Engineering*, vol. 41, no. 8, pp. 3061–3070, 2016, doi: 10.1007/s13369-016-2082-x.
- [32] M. A. Selver, A. Kocaoglu, G. K. Demir, H. Dogan, O. Dicle, and C. Guzelis, "Patient oriented and robust automatic liver segmentation for pre-evaluation of liver transplantation," *Computers in Biology and Medicine*, vol. 38, no. 7, pp. 765–784, Jul. 2008, doi: 10.1016/j.compbiomed.2008.04.006.
- [33] E. Aldemir, G. Tohumoglu, and M. A. Selver, "Binary medical image compression using the volumetric run-length approach," *Imaging Science Journal*, vol. 67, no. 3, pp. 123–135, 2019, doi: 10.1080/13682199.2019.1565695.

## BIOGRAPHIES OF AUTHORS



**Arif Sameh Arif**    was born in Baghdad in 1970, he was obtained a bachelor's degree from Al-Mustansiriya University/College of Science, Department of Mathematics. The master's degree in computer science image processing from the University of Technology. The Ph.D. in computer science image processing from Multimedia University (MMU) Cyberjaya Malaysia. He has nearly 25 years teaching experience in the Department of Computer Science. He is currently work as a lecturer in the Department of Computer Systems Techniques, Institute of Administration Al Russaffa, Middle Technical University, Baghdad, Iraq. He published more than 15 articles in international and national journals and conferences. He can be contacted at email: arifsameh@ieee.org and Dr.ArifSameh2016@mtu.edu.iq.



**Muntaha Abboud Jassim**    was born in Baghdad in 1968, she was obtained a bachelor's degree from Salah al-Din University/College of Administration and Economics Department of Statistics, a master's degree in computer science - Image processing from the University of Technology. She has nearly 11 years teaching experience in the Department of Computer Science. She is currently working as a lecturer at the Basic Science Department, College of Dentistry, Al-Mustansiriya University. She published more than 6 articles in international and national journals and conferences. She can be contacted at email: muntahaabood2006@gmail.com.